Structure and function of Cortical Dysplasias

In a BCNU model

Aquiles, A., Luna-Munguía, H., Concha, L. , Fiordelisio, T. Regalado, M.

Focal cortical dysplasia (FCD) is one of the most frequent causes of refractory focal epilepsy and is currently classified into three main types based on their morphological features upon histopathological examination. Their variability in morphology, location, and extension are major hurdles to early and accurate diagnosis and prognosis. Moreover, it is still unclear which mechanisms drive epileptogenicity in these lesions. Here, we used an animal model of cortical dysplasia (Benardete, Epilepsia 2002; 43, 970-982) to investigate the functional network properties and their response to a hyperexcitable challenge.

Methods

We studied the offspring of pregnant Sprague Dawley rats that were injected with either saline solution (**Control** n=21) or carmustine (**BCNU** n=26) (20 mg/kg i.p.) at 14 days of gestation. Ten animals per group were submitted to anatomical T2-weighted **MRI** at 30, 37, 44, and 51 postnatal days using a 7 T preclinical scanner (resolution = 67x67x80, 80 μm³) to derive cortical thickness at the level of the primary motor cortex (M1) in a coronal slice. To confirm cortical cellular disorganization, we performed layer-specific **immunofluorescence** examinations of M1 in coronal sections of 3 control and 6 BCNU cryopreserved specimens at p30 (Foxp2 for layer VI, Necab for layer IV, and NeuN for neurons). Finally, another group of Control (n=8) and BCNU (n=10) animals were used for *in vitro* **calcium imaging** to assess the activity and organization of intracortical circuits at p30. Brain slices were recorded using a stereoscope fluorescence microscope coupled to a CCD camera. Each brain slice was permeabilized with Fluo-4 AM at atmospheric conditions.

Cell connectivity inference was performed following the principle of cross-correlation between cells. To verify that the possible correlations were non-random, for each record a new dataset of 1000 times simulated time series was constructed, which were also correlated and these surrogate correlation values facilitated the creation of a distribution of values per cell to select those correlations that were non-random in each record (> 2 S.D.). Given the large number of correlations performed, spurious correlations were minimized using the False Discovery Rate method.

In order to evaluate this method in different temporal windows, 5 windows of 150 s each were determined in each correlation (before 0-150s, during (150-300s), after (300-450s, 450-600s, 600-750s)), based on the chronology of the acquisition of the recording and to observe the before, during and after of the hyper-excitable stimulus at the connectivity level.

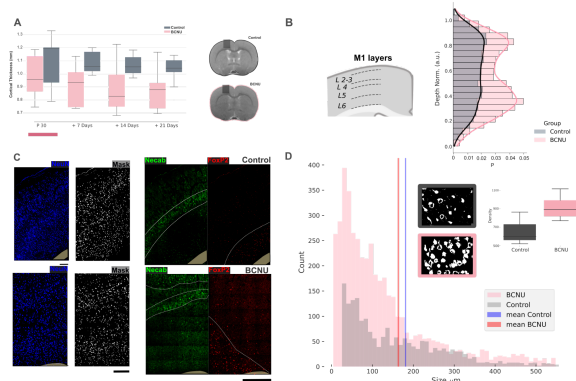### Macro and micro-structure of BCNU and Control cortexes

Figure 1. Macro and micro-structural evaluations in BCNU and Control cortexes. **A.** Group-wise comparison of the longitudinal changes of the cortical thickness in M1 in both groups (pink= BCNU, grey =Control), p < 0.005. **B.** The neuron profiles comparison between both M1 cortexes (BCNU = 5, Control = 3). **C.** Representative immunofluorescence essays, given by the neuron (NeuN), layer IV (Necab), layer VI (FoxP2) marks in both groups. Scale bars 100 um, 300 um. **D.** The size and density of neurons comparison between groups (pink = BCNU (n=5), grey (Control(n=3)). and zoom of one FOV at 150 um.

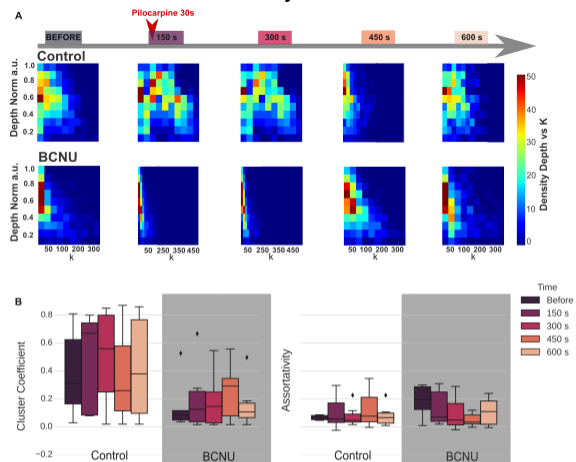### Cell connectivity evolution

Figure 2. Evolution of M1 cortical network before and after an external hyperexcitable stimulus.

A. The evaluation of network degree (k) evolution throughout the different time-points and their relation with cell depth, in a single animal per group. The red arrowhead (within the 150 s window) represents the moment in which the external hyperexcitable stimulus is applied (pilocarpine 300 μM, 30s). The scale bar shows the density of occurrence of each relation value.

B. Group-wise comparison of network metrics: cluster coefficient and assortativity between times and groups

Results

Dysplastic cortexes at an early stage of development (p30) show macrostructural (**Figure 1A**) and microstructural differences characterized by evident delamination and neuronal dispersion (**Figure 1B, C, D**). Functionally, the dysplastic cortices showed a rearrangement of intracortical connectivity after the hyperexcitable stimulus, making them weaker and less connected, without returning to their basal state (**Figure 2A**). Furthermore, they show less stability in their internal network communication after the external hyperexcitable stimulus (**Figure 2B**).

Conclusions

Our results suggest that the disarranged structure of dysplasias may affect intracortical connectivity after an external hyperexcitable stimulus, which reduces their connections and renders them less dynamic.

Acknowledgments